Chemical Engineering Journal 161 (2010) 19–26

Contents lists available at ScienceDirect

Chemical Engineering Journal

journal homepage: www.elsevier.com/locate/cej

Flux decline analysis in micellar-enhanced ultrafiltration of synthetic waste solutions for metal removal

Ruey-Shin Juang[a,b,*], Su-Hsia Lin[c], Li-Chuan Peng[a]

[a] Department of Chemical Engineering and Materials Science, Yuan Ze University, Chung-Li 32003, Taiwan
[b] Fuel Cell Center, Yuan Ze University, Chung-Li 32003, Taiwan
[c] Department of Chemical and Materials Engineering, Nanya Institute of Technology, Chung-Li 320, Taiwan

ARTICLE INFO

Article history:
Received 20 November 2009
Received in revised form 1 April 2010
Accepted 2 April 2010

Keywords:
Flux decline
Micellar-enhanced ultrafiltration
Anionic surfactants
Metal removal
Blocking filtration laws
Specific cake resistance

ABSTRACT

It is known that micellar-enhanced ultrafiltration (MEUF) is an efficient and economic process for the removal of trace metal ions and organics from aqueous media. In this work, flux decline behavior in MEUF of aqueous solutions containing trace Cu(II) (1.6–8 mM) and anionic surfactants sodium dodecyl sulfate (SDS) or sodium dodecyl benzene sulfate (SDBS) was studied at 25 °C in batch mode. An UF membrane that had average pore size comparable to those of Cu(II)-adsorbed micelles was adopted. All experiments were performed as a function of stirring speed (200–400 rpm), solution pH (3.0–5.0), molar concentration ratio of surfactant to metal (S/M, 2.5–12.7), and applied pressure (69–345 kPa). It was shown that more than 90% of Cu(II) could be removed at an S/M ratio of 12.7 and pH 5 using SDS. The blocking filtration law was used to identify the mechanism(s) of flux decline during the MEUF processes. Finally, the specific cake resistances in both SDS and SDBS systems were evaluated and compared.

1. Introduction

Inorganic pollutants are of considerable concern because they are non-biodegradable, highly toxic and cause probable carcinogenic effects. If directly discharged into sewage system they may seriously damage the operation of biological treatment as well as make the activated sludge unsuitable for the application to agricultural land [1]. For the removal of heavy metals from aqueous effluents, the traditional techniques are either incapable of reducing their concentrations to the levels required by law (e.g., process of reduction or lime precipitation) or comparatively expensive (e.g., activated carbon adsorption, process of ion exchange, electrolytic removal). Membrane process becomes today an attractive and suitable technique in the treatment of industrial wastewaters containing toxic heavy metals, and has to be easily included in whole process [2]. This is the reason why membrane separation processes are being used more and more frequently. Moreover, separation can be carried out at room temperature; the surface area of membrane module is easily adjusted to wastewater flows; and various industrial membranes are currently available. To remove heavy metals from aqueous streams, reverse osmosis (RO) or nanofiltration (NF) can be readily used due to the small size of metal ions; however, the flux of RO is limited and requires comparatively high applied pressure [3], or the total rejection by NF is not easily achieved [4], making the process practically unattractive.

Thus, there has been an increasing level of interest and research efforts to improve the performance or reduce the cost of membrane processes. Various forms of surfactant-based membrane separation processes such as micellar-enhanced ultrafiltration (MEUF) [4–6], micellar extraction coupled with UF [7,8], and ion-expulsion UF [9] have been proposed to remove heavy metals from aqueous streams. Of these processes, MEUF has been often used for this purpose in the past decade, particularly from dilute solutions, due to its simplicity and low cost of the operation [4–6,10–12]. Metal ions are adsorbed *via* electrostatic attraction onto surfactant micelles, which formed as surfactant concentration is higher than its critical micelle concentration (cmc), followed by subsequent retention of the metal–micelle complexes by UF. In this regard, the micelles resulting from anionic surfactants are applied for removing positively charged metals. Generally speaking, the efficiency of metal removal depends on the characteristics and concentration ratio of surfactant and metals, solution pH and composition, ionic strength, and the parameters related to membrane unit operations (such as applied pressure, flow rate or stirring speed, and membrane pore size) [4–6,10–16]. Although MEUF has been widely examined, to our best knowledge, most of the previous studies merely focused on the effects of aforementioned system variables on the removal or separation of metal ions. Relatively few studies reported and

* Corresponding author at: Department of Chemical Engineering and Materials Science, Yuan Ze University, 135 Yuan-Tung Road, Chung-Li 32003, Taoyuan, Taiwan. Tel.: +886 3 4638800x2555; fax: +886 3 4559373.
E-mail address: rsjuang@saturn.yzu.edu.tw (R.-S. Juang).

1385-8947/$ – see front matter © 2010 Elsevier B.V. All rights reserved.
doi:10.1016/j.cej.2010.04.007

Nomenclature

A	effective membrane area (m^2)
C_f	Cu(II) concentration in the feed (mM)
C_p	Cu(II) concentration in the permeate (mM)
J	permeate flux of actual solution (L/(m^2 h))
k	constant defined in Eq. (1) (h/m^3)$^{2-n}$
MFI	modified fouling index defined in Eq. (7) (h/m^6)
n	constant defined in Eq. (1)
ΔP	applied pressure (kPa)
r^2	correlation coefficient
R_c	resistance of the cake (m^{-1})
R_m	resistance of the membrane (m^{-1})
S/M	molar concentration ratio of surfactant to metal
SDS	sodium dodecyl sulfate
SDBS	sodium dodecyl benzene sulfate
t	filtration time (h)
V	cumulative permeate volume (m^3)

Greek letters

α	specific cake resistance defined in Eq. (6) (m/kg)
μ	viscosity of the permeate (Pa s)

analyzed the flux decline or fouling behavior of membrane during MEUF [16].

In this work, the flux decline or fouling behavior of a batch MEUF process was analyzed and the specific cake resistance was evaluated. Cu(II) and sodium dodecyl sulfate (SDS) or sodium dodecyl benzene sulfate (SDBS) were selected as model heavy metal and anionic surfactant, respectively. The instantaneous flux and Cu(II) rejection were measured at different molar concentration ratios of surfactant to metal (S/M), solution pH values, stirring speeds, and applied pressures.

2. Model description

The blocking filtration laws derived previously by Hermia [17] are adopted here as a resistance model. It essentially represents the time dependent behavior of cumulative filtrate volume (V) for constant-pressure dead-end membrane filtration [18], which is given by

$$\frac{d^2t}{dV^2} = k\left(\frac{dt}{dV}\right)^n \quad (1)$$

where k and n are the parameters, which depend on the characteristics of particle and filtration medium. The physical meaning of n value of 0, 1, 1.5, and 2, as shown in Fig. 1 [19], corresponding to the mechanism of cake filtration, intermediate blocking, standard blocking, and complete blocking, respectively, is described as follows:

(a) Cake filtration

Ideal cake filtration is based on the assumption that all particles are accumulated in a cake layer. Also, it is assumed that the cake resistance is proportional to the thickness of the cake.

(b) Intermediate blocking

In the intermediate blocking law, particles are allowed to settle on previously deposited particles. It is assumed that each location has an equal probability of being occupied. This means that the chance that a particle settles on a free site is equal to the ratio of free and occupied sides. It is assumed that blocked pores are impermeable.

(c) Standard blocking

The standard blocking law is based on the assumption that all particles settle inside the pores. Hence, the occupied pore volume is

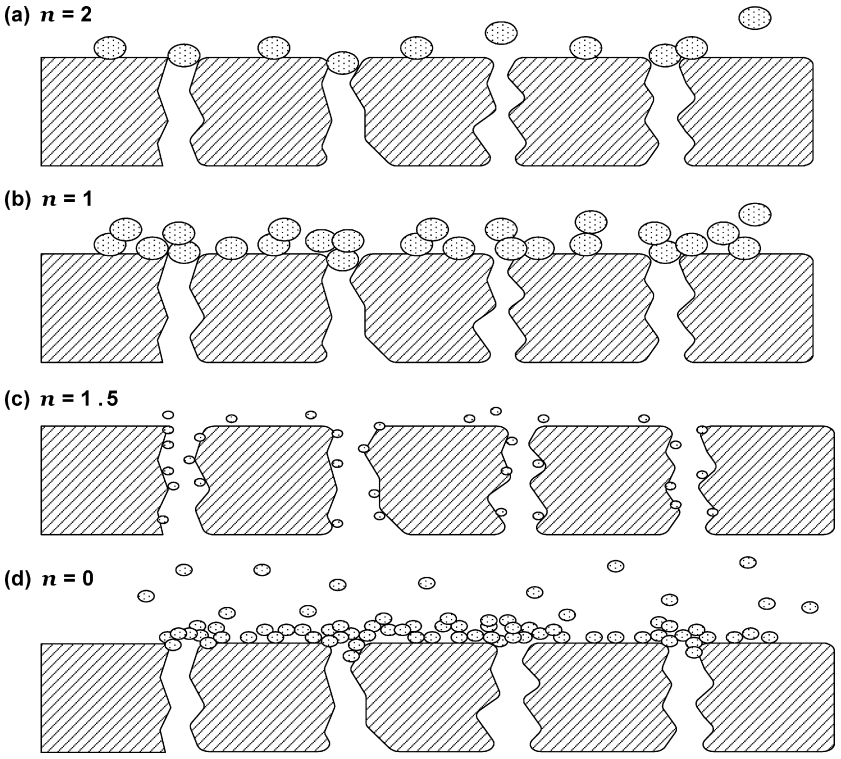

Fig. 1. Schematic diagrams of the blocking filtration laws: (a) complete blocking, (b) intermediate blocking, (c) standard blocking, and (d) cake filtration [19].

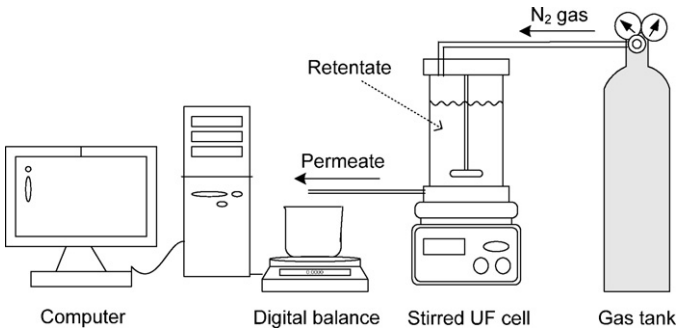

Fig. 2. Schematic diagram of the experimental setup of dead-end UF process.

proportional to the filtrated volume. The Hagen–Poissuille equation is used to relate the pore volume (diameter) to the resistance.

(d) Complete blocking

It is assumed that each filtrated particle participates in blocking the membrane. Hence, the blocked area depends linearly on the filtrated volume. Furthermore, it is assumed that blocked parts of the membrane are impermeable. Consequently, the resistance is inversely proportional to the fraction of free pores.

In principle, any other real value of n can be allowed; however, there is no physical interpretation in that case. The constant k can be explained as a scaling factor that is proportional to the concentration of foulants. The parameter n can be easily identified by fitting the measured data; for example, the plots of $\ln V$ versus t, t/V versus V, V versus $\ln t$, and t/V versus t will give a straight line for $n = 2$, 0, 1, and 1.5, respectively [17].

3. Materials and methods

3.1. Reagents and solutions

The surfactants sodium dodecyl sulfate (SDS) was purchased from ACROS Co. and sodium dodecyl benzene sulfate (SDBS) was obtained from Sigma–Aldrich Co. Both surfactants were diluted with deionized water (Millipore, Milli-Q), to which an amount of $CuSO_4$ was added. Otherwise indicated elsewhere, 20 mM of SDS or SDBS was used throughout this work because the cmc of SDS and SDBS was measured to be 8.0 and 1.8 mM, respectively (not shown). Solution pH was adjusted by adding a small amount of 0.1 M NaOH or H_2SO_4, which was measured using a digital pH meter (Horiba F-23, Japan). All inorganic chemicals were of analytical reagent grade (Merck Co., Germany) and used as received.

3.2. Dead-end UF experiments

Fig. 2 illustrates the experimental setup. The UF experiments were performed in a batch stirred cell (Millipore, XFUF07601) with a capacity of 300 mL, where the disc membrane has a diameter of 76 mm with a geometric area of 41.8 cm^2. The applied pressure (ΔP) of UF cell was controlled by nitrogen gas. The stirring speed varied in the range 200–400 rpm. Experiments were carried out at around 25 °C controlled by air conditioning. The membrane YM10 (Amicon Co.) with molecular weight cut-off (MWCO) of 10,000 was used here, which is made of regenerated cellulose.

The instantaneous permeate flux (J) at each run was calculated in the time intervals t_1 and t_2 by

$$J = \frac{(V_2 - V_1)}{A\,(t_2 - t_1)} \tag{2}$$

where A is the effective membrane area (m^2). Also, the average rejection of Cu(II) was obtained as follows:

$$\text{rejection} = 1 - \frac{C_p}{C_f} \tag{3}$$

where C_p and C_f were the concentrations of Cu(II) in the permeate and feed, respectively, at pseudo-steady state. The typical time profiles of filtration flux J over the entire process can be empirically expressed in the following exponential dependence [20]:

$$J = \sum_{i=1}^{p} (J_{i-1} - J_i)\exp(-k_i t) + J_i \tag{4}$$

Here the steady flux was obtained at $t \to \infty$ through the selection of r such that the percent of standard deviation between the fitted and measured flux was less than 1% (in most cases, $p = 2$–4). The samples were taken from the permeate at preset time intervals and the concentrations of Cu(II) were analyzed by a Varian atomic absorption spectrophotometer (Model 220FS).

The rejection of 20 mM SDS or SDBS micelles in the absence of Cu(II) with YM10 was also measured by the similar procedures to those of Cu(II) as described above. The concentrations of SDS and SDBS in the solutions were determined by a Shimadzu UV/vis spectrophotometer (Model UV-240) [14,21].

3.3. Micelle size measurements

In this work, the electrophoretic mobility of the solution containing Cu(II)-adsorbed micelles (that is, before MEUF experiments) was determined with a Zetasizer 3000HS analyzer (Malvern, UK). Each sample was analyzed three times, and the information about size distribution by intensity and by volume as well as the total intensity was recorded.

3.4. Regeneration of used membranes

After the completion of each experiment, the membrane used was cleaned in ultrasonic cleaner with 0.1 M NaOH for 30 min once and then with deionized water twice. The pure water flux was then measured. The integrity and performance of the membrane was considered to be maintained if pure water flux was within 95% of the virgin membrane. The cleaned membranes were stored in 0.05% sodium azide solution at 4 °C.

4. Results and discussion

4.1. Effects of operating parameters on Cu(II) rejections

Figs. 3 and 4 show the effect of applied pressure (ΔP) on Cu(II) rejection. The rejection increases with increasing ΔP, which is likely due to the formation of thicker cake at higher applied pressures. This behavior was observed previously. For example, Ahmad and Puasa [22] have found that there is an increased trend in rejection of cetylpyridinium chloride, a cationic surfactant, when the operating pressure increases. However, Akita et al. [13] have reported that a pressure rise causes an increase in flux without affecting the rejection of Au(III) with nonionic surfactant polyoxyethylene nonyl phenyl ether in the range measured. It is likely that the fouling of ionic surfactants is affected more significantly by the pressure due to the stronger electrostatic interactions. The effect of solution pH on Cu(II) rejection is also shown in Figs. 3 and 4. An increase in Cu(II) rejection is found when pH increases. This is because more H^+ competitively adsorbs on negatively charged micelle surfaces at lower pH [14]. Akita et al. [8] have observed that increasing pH enhances metal rejection with 2-ethylhexyl

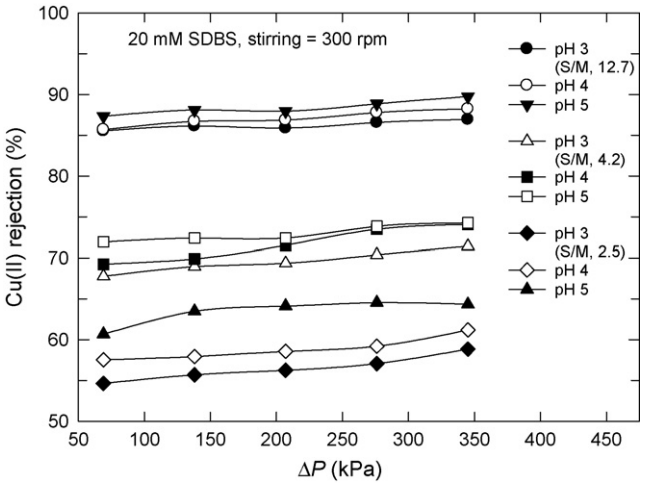

Fig. 3. Effect of applied pressure on Cu(II) rejection with SDBS by MEUF.

phosphonic acid monmo-2-ethylhexyl ester solubilized by polyoxyethylene nonyl phenyl ether, and nearly complete rejection of Co(II) is attained from aqueous solutions at pH higher than 5.5; whereas, neither metal is rejected from solutions below pH 3.0.

The effect of molar concentration ratio of surfactant to metal (S/M) on Cu(II) rejection is also depicted in Figs. 3 and 4. As expected, higher Cu(II) rejection is obtained at higher S/M ratios due to the more micellar surface available for metal adsorption. Huang et al. [5] have indicated that two important criteria, namely surfactant concentrations of greater than its cmc and S/M ratio of greater than a certain value, have to be met to achieve efficient metal removal efficiency by MEUF. It is noticed that in the absence of SDS or SDBS the rejection of Cu(II) by YM10 in the pH range 3–5 is less than 2% at ΔP = 207 kPa (not shown). Our previous study [15] also found that in the pH range 2–6 the Cu(II) chelate of ethylenediaminetetraacetic acid almost passes through YM10 (rejection < 6%).

In comparison with Cu(II) rejection with the two surfactants, higher rejection is found when SDS is used (Figs. 3 and 4). This is likely because the size of the metal-adsorbed SDS micelles is slightly larger than that of the SDBS micelles as shown in Table 1. The average pore size of YM10 membrane is 5 nm, whereas the average sizes of the Cu(II)-adsorbed SDS and SDBS micelles are 5.3–5.5 nm (polydispersity, 33–38%) and 4.8–5.4 nm (polydispersity, 29–36%), respectively. Accordingly, the MEUF process with SDS should have

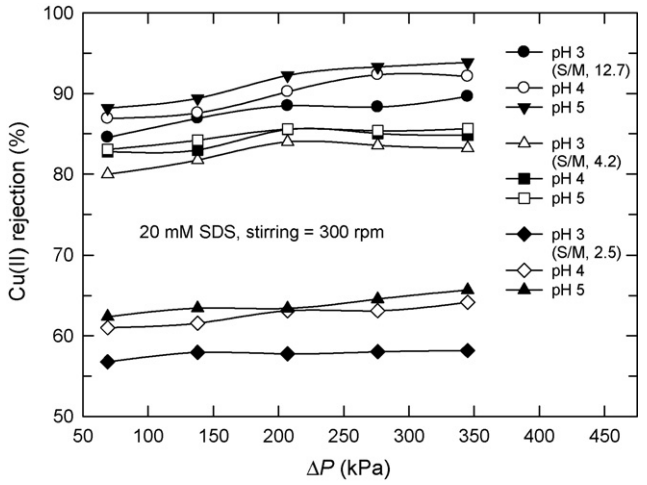

Fig. 4. Effect of applied pressure on Cu(II) rejection with SDS by MEUF.

Table 1
Average size of the Cu(II)-adsorbed surfactant micelles (in nm).

pH	SDBS			SDS		
	S/M = 12.7	S/M = 4.2	S/M = 2.5	S/M = 12.7	S/M = 4.2	S/M = 2.5
5.0	5.4	5.0	4.9	5.5	5.5	5.4
4.0	5.4	4.9	4.9	5.4	5.3	5.3
3.0	5.3	4.8	4.8	5.4	5.3	5.3

higher Cu(II) rejection than with SDBS under comparable conditions.

4.2. Effects of operating parameters on UF fluxes

Fig. 5 shows that the flux slightly increases with increasing stirring speed. This can be understood that vigorous agitation makes large shear stress, thereby reducing the potential of membrane fouling. A stirring speed of 300 rpm was selected here because in this case a serious vortex within the cell was avoided. The effects of solution pH, S/M ratio, and ΔP on the steady fluxes are shown in Figs. 6 and 7. Evidently, the flux increases linearly with increasing ΔP at high S/M ratios with SDBS (Fig. 6a); however, such linear trends are not found at lower S/M ratios as shown in Fig. 6b and c. The possible reason is that the average size of the micelles at lower S/M ratios is smaller than that at higher S/M ratios (Table 1). The SDBS micelles with a size of 4.8 nm formed at low S/M ratios may tend to more easily block into the membrane pores (5 nm). This argument is supported by the results of Fig. 8, which show that the flux due to the presence of SDS micelles decreases with time more gradually and smoothly than that of SDBS micelles under comparable conditions (e.g., 20 mM) [23].

On the other hand, the effect of solution pH on the flux can be neglected. This is because the sizes of the micelles are nearly identical at all pH values studied. Also, it is found that the flux increases linearly with increasing ΔP with SDS (Fig. 7). This is not wholly the case with SDBS, particularly at S/M ratios smaller than 4.2. That is, there exists a ΔP in that curve that a further increase in ΔP can no longer improve the flux; the corresponding flux is the so-called limiting flux [24]. Evidently, the limiting flux decreases with decreasing S/M ratio. Decreasing S/M ratio means that the micelle surface is less negatively charged when surfactant concentration is fixed at 20 mM; making the repulsive force between metal–micelle complex and membrane surface rather weaker. It should be noted that the size of the Cu(II)–SDBS micelles at S/M ratios smaller than

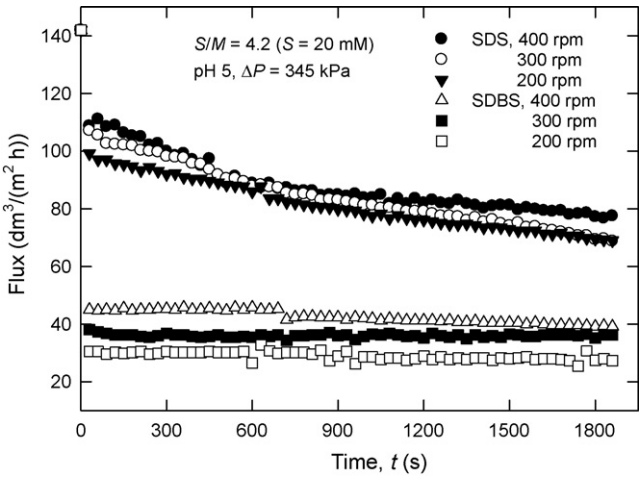

Fig. 5. Effect of stirring speed on the variations of fluxes with time at an S/M ratio of 4.2 and pH 5.

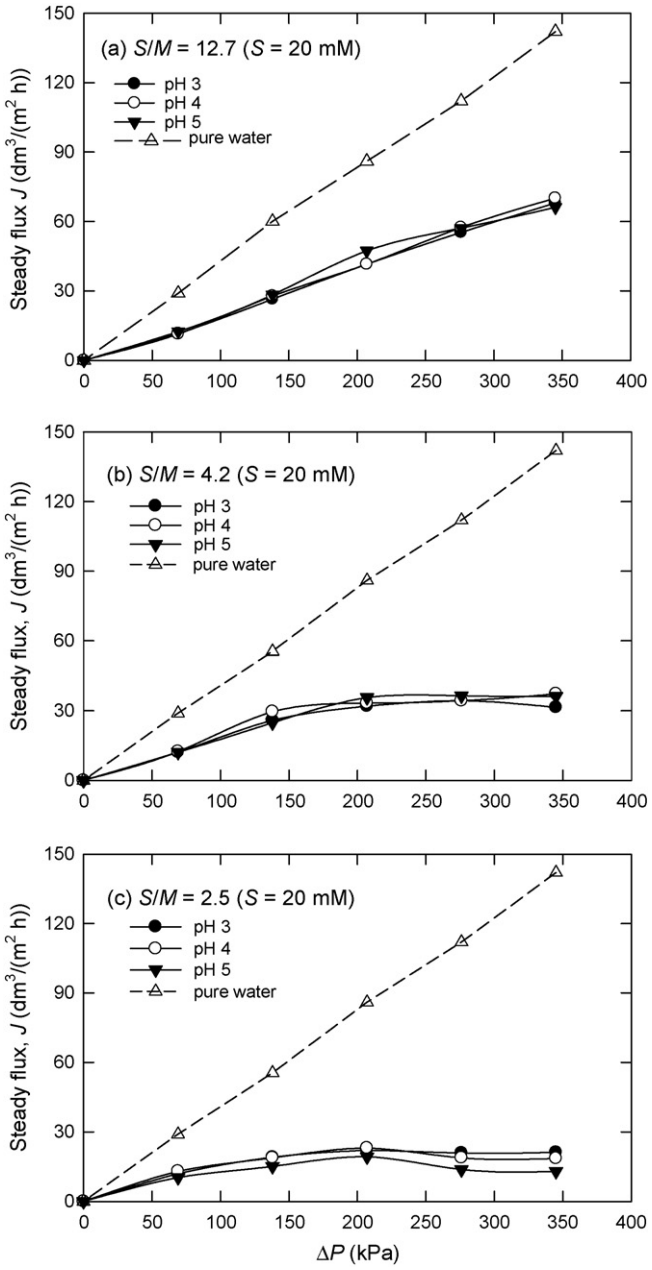

Fig. 6. Effect of applied pressure on the steady flux with SDBS at a stirring speed of 300 rpm and different pH values and S/M ratios.

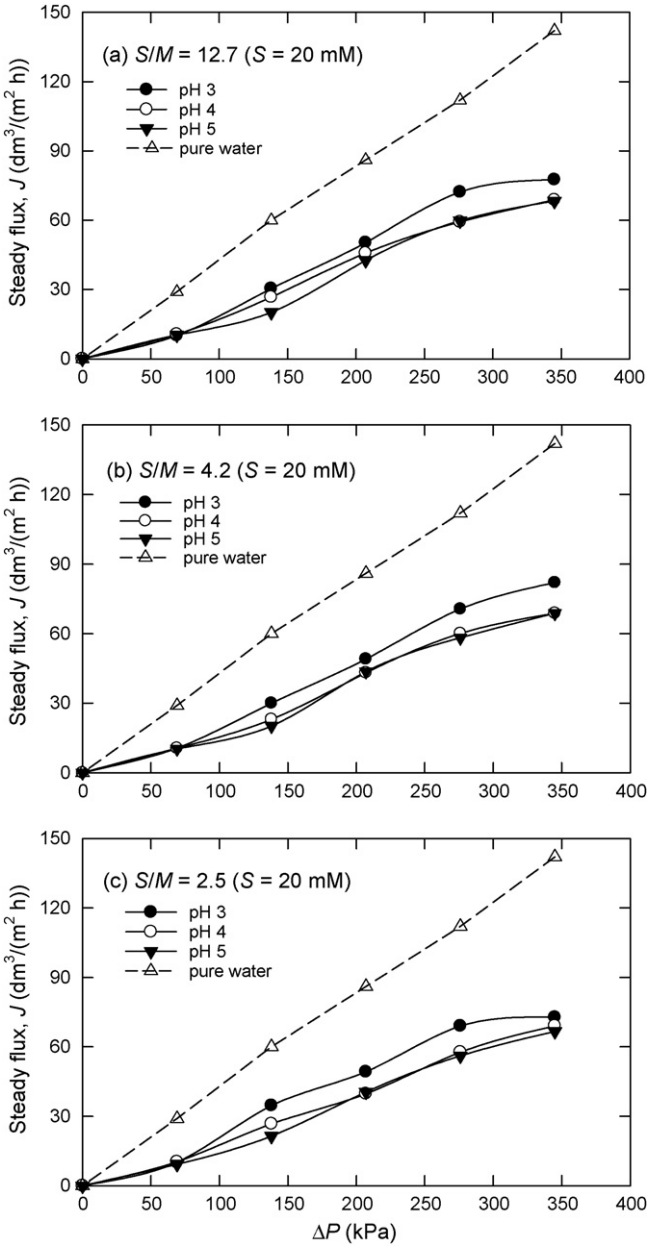

Fig. 7. Effect of applied pressure on the steady flux with SDS at a stirring speed of 300 rpm and different pH values and S/M ratios.

4.2 is all less than the size of membrane pores (5 nm) as shown in Table 1.

A steady flux of 85 $dm^3/(m^2\,h)$ obtained in this work under the conditions of ΔP = 345 kPa, pH 5, and S/M = 12.7 with YM10 (Fig. 7a) closes to 88 $dm^3/(m^2\,h)$ obtained under the conditions of ΔP = 400 kPa and 8 mM SDS with UPM20 membrane [25] and is larger than 18 $dm^3/(m^2\,h)$ obtained under the conditions of ΔP = 50 kPa and 0.01 M polyoxyethylene nonyl phenyl ether with YM10 [13]. However, the rejections of those metals including Cu(II), Ni(II) [21], and Au(III) [13] are comparable and are in the range 83–89%.

4.3. Mechanism of flux decline

In principle, typical filtration has three regions in which pore blocking, cake filtration, and cake filtration with compression, take place consecutively [23]. In the first region, the deposition of particles blocking the entry to a pore or inside membrane pore causes a sharp increase in slope. This is followed by a minimum linear slope where particles deposit on the membrane surface. The modified fouling index (MFI) is based on cake filtration (region 2); particles are retained on the membrane surface as a cake. This is demonstrated in Figs. 9a and 10a. The cake adds additional resistance (R_c) to the resistance of membrane (R_m), and the flux decline under constant pressure filtration can be described as follows [24]:

$$\frac{dV}{Adt} = \frac{\Delta P}{\mu(R_m + R_c)} \tag{5}$$

where t is the filtration time (h) and μ is the viscosity of the permeate (Pa s).

Graphical tests (Figs. 9a or 10a) prove that there is no cake compression (the last region) in our systems. The resistance of cake, assuming the retention of particles is constant, is hence propor-

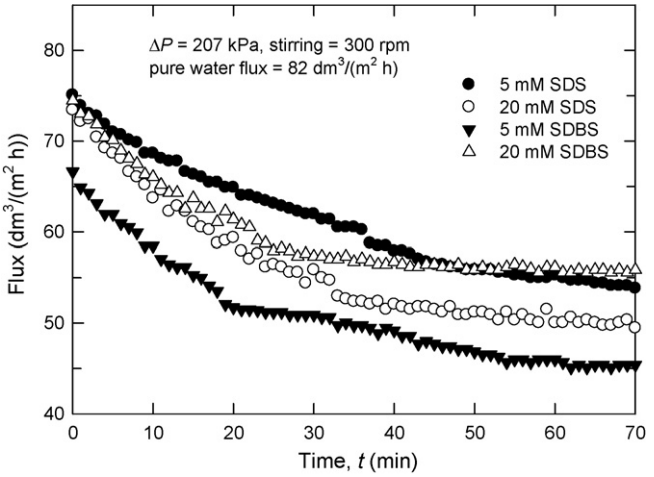

Fig. 8. Variations of the fluxes of pure SDS and SDBS solutions with time at ΔP = 207 kPa.

tional to the amount of cake deposited at the membrane and the fouling tendency of feed water expressed as the fouling index, αC.

$$R_c = \frac{V\alpha C}{A} \tag{6}$$

where α is the specific cake resistance (m/kg). Combining Eqs. (5) and (6), followed by integration at constant pressure gives the known cake filtration equation (n = 0):

$$\frac{t}{V} = \frac{\mu R_m}{\Delta PA} + \left(\frac{\mu\alpha C}{2\ \Delta PA^2}\right) V \tag{7}$$

Therefore, a plot of (t/V) versus V should give a straight line with slope equal to ($\mu\alpha C/2\Delta PA^2$), which is referred to the MFI, as shown and justified in the latter stage of filtration in Figs. 7a and 8a for SDBS and SDS systems, respectively (correlation coefficient $r^2 > 0.9852$).

The specific cake resistance, α, is often used to characterize the hydrodynamic resistance of cake during the filtration of particulate suspensions [25]. Tables 2 and 3 list the calculated α values for SDBS and SDS systems, respectively. It is found that α increases with increasing S/M ratio and pH, particularly for SDBS system. Under the pH range studied, α decreases initially and then increases with increasing ΔP for SDBS system; however, α always decreases with increasing ΔP for SDS system except when ΔP = 138 kPa. It is likely that the formation of cake is slower at lower ΔP, leading to high α value. Such trends are inconsistent with those reported previously [26–28]. For example, McCarthy et al. [27] have found that there is a linear relationship between α and ΔP over the whole range of pressures for all broths examined with compressible cake. Lodge et al. [28] have studied the characterization of dead-end UF of biotreated domestic wastewater and found that the cake is highly compressible; specific cake resistance increases by an order of magnitude

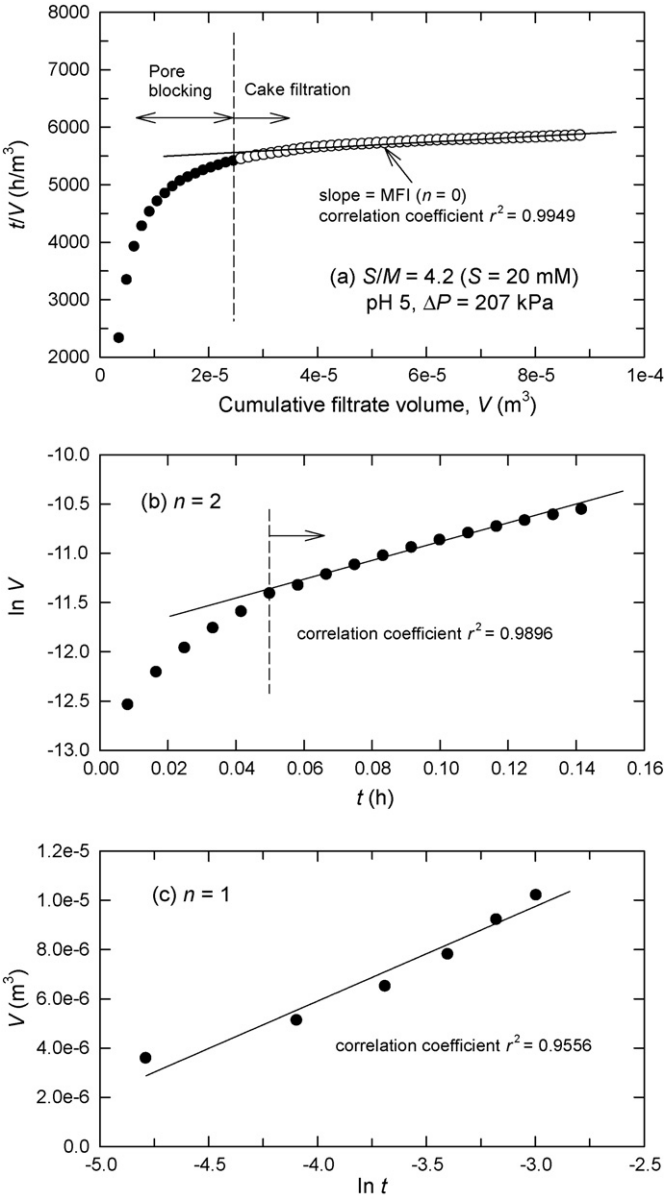

Fig. 9. Plots of (a) t/V versus V during the whole MEUF with SDBS under the conditions of S/M = 4.2, ΔP = 207 kPa, and pH 5 as well as (b) ln V versus t and (c) V versus ln t at the initial stage of the process.

Table 2
The specific cake resistance α in the MEUF of Cu(II) solutions with SDBS (in 10^7 m/kg).

S/M ratio	pH	ΔP (kPa)				
		345	276	207	138	69
12.7	3.0	20	17	36	66	136
	4.0	30	25	45	80	137
	5.0	325	260	208	156	139
4.2	3.0	18	15	32	46	134
	4.0	24	22	38	52	135
	5.0	65	53	39	56	138
2.5	3.0	16	13	30	41	130
	4.0	18	14	32	42	132
	5.0	42	37	26	44	135

Table 3
The specific cake resistance α in the MEUF of Cu(II) solutions with SDS (in 10^7 m/kg).

S/M ratio	pH	ΔP (kPa)				
		345	276	207	138	69
12.7	3.0	11	14	25	26	263
	4.0	17	21	34	78	265
	5.0	23	25	41	104	268
4.2	3.0	10	13	23	26	261
	4.0	16	20	29	78	262
	5.0	20	23	39	104	265
2.5	3.0	9.2	11	22	26	257
	4.0	15	18	26	78	259
	5.0	18	20	35	104	263

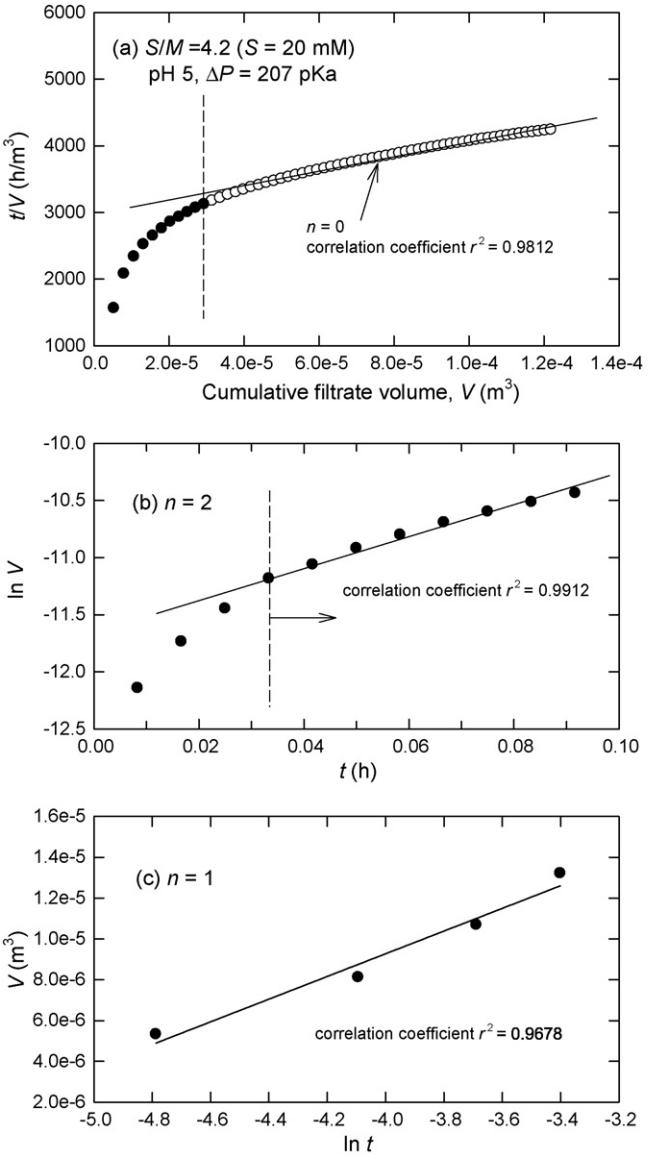

Fig. 10. Plots of (a) t/V versus V during the whole MEUF with SDS under the conditions of S/M = 4.2, ΔP = 207 kPa, and pH 5, as well as (b) ln V versus t and (c) V versus ln t at the initial stage of the process.

when ΔP increases from 12.7 to 100 kPa. Possibly, the compressibilities of particulates are different among these solutes. The reasons leading to such discrepancies are unavailable at this stage; the use of YM10 is a possible reason because the average sizes of membrane pores and Cu(II)-adsorbed micelles are equivalent. Also, this is possibly due to dead-end configuration; most of the micelles have been already deposited onto the membrane by the time the cake formation regime was reached, especially at lower pressures, when this point is reached later.

Cornelis et al. [29] studied the effect of the MWCO and contact angle of NF membrane on the flux of nonionic surfactant solution at a concentration lower that its cmc. They have indicated that the adsorption of surfactant on the surface or within the pore of the membrane plays a crucial role in flux behavior. When the MWCO is slightly lower or comparable to the size of surfactant monomer, monomers can penetrate the pores. As the membrane is comparatively hydrophobic, strong adsorption of the monomers occurs and the pore radius is reduced, leading to flux decline. Much less strong adsorption results in a limited flux decline. As the MWCO is much lower than the monomer size, however, monomers cannot penetrate the pores and flux is affected only by changes to membrane surface. On hydrophobic membrane groups, strong irreversible adsorption of hydrophobic surfactant tails occurs, which improves the wettability of the surface, whereas on hydrophilic membrane groups, the hydrophilic heads are adsorbed and the wettability is reduced. Depending on the hydrophilicity of the membrane, the net effect is flux increase or decrease. In the present system, the limited flux decline behavior with SDBS (Fig. 6b and c) implies that much weak adsorption of the micelles occurs and pore radius is not considerably reduced [29,30]. It appears that the role of pore blocking in the UF of SDBS micelles is not significant according to the flux decline behavior of SDBS micelles (Fig. 8). In fact, the rejection of pure SDS or SDBS micelles (20 mM) by YM10 is measured to be above 90%, likely due to the existence of the cake layer [14,30].

At the initial stage of filtration, as shown in Figs. 9a and 10a, the type of pore blocking should be further indentified to be either intermediate blocking (n = 1), standard blocking (n = 1.5), complete blocking (n = 2), or the combination. In practice, evident deviations between the measured and fitted results are observed (not shown) by adopting any single n value. This implies that more than one types of blocking mechanisms are involved even at the early stage of the process. The multiple fitting is most satisfactory in both SDBS and SDS systems when n = 1 and the followed n = 2 are adopted, as shown in Figs. 9b and c, 10a and b. Based on the fact that the average size of membrane pores is comparable to that of the Cu(II)-adsorbed micelles, the intermediate and complete blocking mechanisms consecutively play a crucial role in the initial flux decline [15]. Thus, the flux decline mechanism in the present MEUF process is that in the early stage of process each micelle particle participates in blocking the pores of the membrane and the blocked parts of the membrane are impermeable mainly according to the intermediate and complete blocking mechanisms, and all micelles are accumulated to form a cake layer in the followed stage of process.

5. Conclusions

Micellar-enhanced ultrafiltration (MEUF) of trace Cu(II) from aqueous streams has been studied at 25 °C with the help of anionic surfactants SDS and SDBS. Removal of Cu(II) higher than 90% could be achieved by regenerated cellulose YM10 membrane (pore size 5 nm) at a molar concentration ratio of surfactant to metal (S/M) of 12.7 and pH 5 with SDS. It was shown that the average size of Cu(II)-adsorbed surfactant micelles played a crucial role in flux decline behavior (5.3–5.5 nm for SDS; 4.8–5.4 nm for SDBS), at least together with the use of YM10. The flux decline in the present MEUF process could be easily analyzed when it was divided into two stages according to the blocking filtration laws. Each micelle took part in blocking the membrane pores at the early stage of the process and the blocked parts of the membrane were impermeable via intermediate blocking mechanism first and then complete blocking mechanism; finally all the micelles were accumulated to form a cake layer in the followed stage of process.

References

[1] P. Madoni, D. Davoli, G. Gorbi, L. Vescovi, Toxic effect of heavy metals on the activated sludge protozoan community, Water Res. 30 (1996) 135–141.
[2] A.K. Pabby, A.M. Sastre, Membrane applications in industrial waste management, environmental engineering and future trends in membrane science: introduction, in: Handbook of Membrane Separations: Chemical, Pharmaceutical, Food, and Biotechnological Applications, CRC Press, Boca Raton, FL, USA, 2008, Part III.
[3] U. Ipek, Removal of Ni(II) and Zn(II) from an aqueous solution by reverse osmosis, Desalination 174 (2005) 161–169.
[4] T. Balanyaa, J. Labandab, J. Llorensb, J. Sabate, Separation of metal ions and chelating agents by nanofiltration, J. Membr. Sci. 345 (2009) 31–35.

[5] Y.C. Huang, B. Batchelor, S.S. Koseoglu, Crossflow surfactant-based ultrafiltration of heavy metals from waste streams, Sep. Sci. Technol. 29 (1994) 1979–1998.
[6] J. Iqbal, H.J. Kim, J.S. Yang, K. Baek, J.W. Yang, Removal of arsenic from groundwater by micellar-enhanced ultrafiltration (MEUF), Chemosphere 66 (2007) 970–976.
[7] I. Escudero, M.O. Ruiz, J.M. Benito, J.L. Cabezas, D. Dominguez, J. Coca, Recovery of α-phenylglycine by micellar extractive ultrafiltration, Chem. Eng. Res. Des. 84 (2006) 610–616.
[8] S. Akita, L.P. Sastillo, S. Nii, K. Takahashi, H. Takeuchi, Separation of Co(II)/Ni(II) via micellar-enhanced ultrafiltration using organophosphorus acid extractant solubilized by nonionic surfactant, J. Membr. Sci. 162 (1999) 111–117.
[9] D.K. Krehbiel, J.F. Scamehorn, R. Ritter, S.D. Christian, E.E. Tucker, Ion-expulsion ultrafiltration to remove chromate from wastewater, Sep. Sci. Technol. 27 (1992) 1775–1787.
[10] J. Landaburu-Aguirre, V. Garcia, E. Pongracz, R.L. Keiski, Removal of zinc from synthetic wastewater by micellar-enhanced ultrafiltration: statistical design of experiments, Desalination 240 (2009) 262–269.
[11] C.K. Liu, C.W. Li, C.Y. Lin, Micellar-enhanced ultrafiltration process (MEUF) for removing copper from synthetic wastewater containing ligands, Chemosphere 57 (2004) 629–634.
[12] E. Samper, M. Rodriguez, M.A. De la Rubia, D. Prats, Removal of metal ions at low concentration by micellar-enhanced ultrafiltration (MEUF) using sodium dodecyl sulfate (SDS) and linear alkylbenzene sulfonate (LAS), Sep. Purif. Technol. 65 (2009) 337–342.
[13] S. Akita, Y. Li, H. Takeuchi, Micellar-enhanced ultrafiltration of gold(III) with nonionic surfactant, J. Membr. Sci. 133 (1997) 189–194.
[14] R.S. Juang, Y.Y. Xu, C.L. Chen, Separation and removal of metal ions from dilute solutions using micellar-enhanced ultrafiltration, J. Membr. Sci. 218 (2003) 257–267.
[15] R.S. Juang, M.N. Chen, Removal of copper(II) chelates of EDTA and NTA from dilute aqueous solutions by membrane filtration, Ind. Eng. Res. Chem. 36 (1997) 179–186.
[16] U. Danis, C. Aydiner, Investigation of process performance and fouling mechanisms in micellar-enhanced ultrafiltration of nickel-contaminated waters, J. Hazard. Mater. 162 (2009) 577–587.
[17] J. Hermia, Constant pressure blocking filtration laws: application to power-law non-Newtonian fluids, Trans. I. Chem. E 60 (1982) 183–187.
[18] P.H. Hermans, H.L. Bredee, Principles of the mathematical treatment of constant-pressure filtration, J. Soc. Chem. Ind. 55T (1936) 1–11.
[19] B. Blankert, B.H.L. Betlem, B. Roffel, Dynamic optimization of a dead-end filtration trajectory: blocking filtration laws, J. Membr. Sci. 285 (2006) 90–95.
[20] M. Mondor, B. Girad, C. Moresoli, Modeling flux behavior for membrane filtration of apple juice, Food Res. Intern. 33 (2000) 539–548.
[21] F. Rusconi, E. Valton, R. Nguyen, E. Dufourc, Quantification of sodium dodecyl sulfate in microliter-volume biochemical samples by visible light spectroscopy, Anal. Biochem. 295 (2001) 31–37.
[22] A.L. Ahmad, S.W. Puasa, Reactive dyes decolorization from an aqueous solution by combined coagulation/micellar-enhanced ultrafiltration process, Chem. Eng. J. 132 (2007) 257–265.
[23] J.C. Schippers, J. Verdouw, The modified fouling index, a method of determining fouling characteristics of water, Desalination 32 (1980) 137–148.
[24] L. Song, A new model for the calculation of the limiting flux in ultrafiltration, J. Membr. Sci. 144 (1998) 173–185.
[25] L. Yurlova, A. Kryvoruchko, B. Kornilovich, Removal of Ni(II) from wastewater by micellar-enhanced ultrafiltration, Desalination 144 (2002) 255–260.
[26] G. Akay, B. Keskinler, A. Cakici, U. Danis, Phosphate removal from water by red mud using crossflow microfiltration, Water Res. 32 (1998) 717–726.
[27] A.A. McCarthy, D.G. O'Shea, N.T. Murray, P.K. Walsh, G. Foley, Effect of cell morphology on dead-end filtration of the dimorphic yeast *Kluyveromyces marxianus* var. marxianus NRRLy2415, Biotechnol. Prog. 14 (1998) 279–285.
[28] B. Lodge, S.J. Judd, A.J. Smith, Characterization of dead-end ultrafiltration of biotreated domestic wastewater, J. Membr. Sci. 231 (2004) 91–98.
[29] G. Cornelis, K. Boussu, B.V. der Bruggen, I. Devreese, C. Vandecasteele, Nanofiltration of nonionic surfactants: effect of the molecular weight cutoff and contact angle on flux behavior, Ind. Eng. Chem. Res. 44 (2005) 7652–7658.
[30] L. Song, Flux decline in crossflow microfiltration and ultrafiltration: mechanisms and modeling of membrane fouling, J. Membr. Sci. 139 (1998) 183–200.